LES OF HEAT TRANSFER IN PIPE FLOW OF POWER-LAW FLUIDS

Paulin Sourou GNAMBODE[1], Meryem OULD-ROUIS[1,*], Xavier NICOLAS[1], Paolo ORLANDI[2]

[1]Université Paris-Est, Laboratoire Modélisation et Simulation Multi Echelle,
MSME UMR 8208 CNRS, 5 bd Descartes, 77454 Marne-la-Vallée, France.
[2]Dipartimento di Ingegneria Meccanica e Aerospaziale, Università La Sapienza, Rome, Italy
[*]*Corresponding author: Meryem.Ould@u-pem.fr*

Abstract

Heat transfer of turbulent forced convection of power-law fluids, flowing in a heated horizontal pipe at isoflux conditions, is numerically analyzed by Large Eddy Simulations (LES), with the extended Smagorinsky model, for various power law indices ($0.75 \le n \le 1.2$) at different Reynolds and Prandtl numbers ($4000 \le Re_s \le 12000$ and $1 \le Pr_s \le 100$) for a non-thermally-dependent fluid, at Pearson number Pn=0. A thermally-dependent fluid is also considered for the case n=0.75, at Re_s=4000 and Pr_s=1, for different Pearson numbers ($0.5 \le Pn \le 5$). To validate the present computations, the LES predictions are compared to the results reported in the open literature for the Nusselt number correlations at Pn=0. The LES predictions also allow a better understanding of the physical mechanisms involved in non-newtonian thermally-dependent fluid flows: with increasing Pn, the relative viscosity is enhanced towards the pipe center while the friction factor and the Nusselt number are significantly reduced.

Keywords

LES, non-newtonian, power-law fluids, turbulent, pipe flow, heat transfer.

1. Introduction

The turbulent flows of non-newtonian fluids are of importance in the mechanical and engineering fields. They are encountered in a wide range of engineering applications. While the turbulence theory, the mathematical models and the numerical methods are well-advanced for newtonian fluids, those for non-newtonian fluids are not as developed. The development of computational models for non-newtonian fluid flows and heat transfer can help to bridge the gap in the existing literature and can contribute to the development of general theories on the turbulent flows of such fluids.

The Pearson number is a dimensionless number that measures the effect of the temperature change on the effective viscosity or consistency of a non-newtonian fluid. When the Reynolds, Prandtl and Pearson numbers are significantly large, large eddy simulation (LES) provides an effective tool to predict the effect of the flow parameters on the turbulent fields. There are very few investigations employing LES for non-newtonian fluids [1,2]. Ohta and Miyashita [1] developed a turbulence model that can reproduce DNS results in non-newtonian fluid flows. They performed LES with a Smagorinsky model, extended according to their DNS results, and showed that it can more accurately predict the velocity of turbulent flows for fluids described by Casson's and power-law models (for flow indices n=0.85 and

n=1.15) than the standard Smagorinsky model. Gnambode et al. [2] used this extended Smagorinsky model to predict the turbulent pipe flow of power law fluids, for various flow indices (0.5<n<1.4), different Reynolds numbers (4000<Re_s<12000) and Prandtl numbers (1<Pr_s<100). Heat transfer in turbulent pipe flow of non-newtonian fluid has been very few studied using Large Eddy Simulations (LES). Some theoretical and experimental works focused on the turbulent heat transfer in pipe flows of non-newtonian fluids for a constant viscosity case. Quaresma and Lima [3] performed an analytical study of heat transfer in turbulent forced convection of pseudoplastic fluids in thermally developing pipe flows under isoflux conditions. They focused on the effects of the Reynolds and Prandtl numbers as well as the power law indices on the temperature profiles and the Nusselt numbers along the thermal entry zone and the fully developed regions. They found that Nusselt number increases with increasing Prandtl or Reynolds numbers, while it decreases with increasing the flow index. Gnambode et al. [4] conducted LES for power law fluids in heated turbulent pipe flows, with the extended Samgorinsky model, using a constant turbulent Prandtl number. They confirmed the suitability of the employed LES approach for such simulations.

It is important to note that for many industrial processes, large temperature differences occur between the wall and the fluid and its viscosity decreases significantly with increasing temperature. In these situations, the flow characteristics change substantially compared with the constant viscosity case and a constant viscosity assumption leads to wrong estimations of the friction and heat transfer coefficients. Thus, it is useful and interesting to consider the effect of the temperature varying viscosity on the turbulent flow and thermal field. However, very few studies account for the dependent viscosity observed in applications. Experiments on the laminar and turbulent flows of a pseudoplastic fluid (n=0.7) in a pipe subjected to a uniform wall heat flux, with temperature dependent viscosity, have been published by Scirocco et al. [5]. For the turbulent regime, the established correlations remain valid as long as the generalized definitions of the Reynolds and Prandtl numbers are used. Peixinho [6] conducted an experimental investigation related to the laminar, transitional and turbulent flows of various non-newtonian fluids, especially Herschell-Bulkey fluids, to investigate the thermal convection in circular and annular pipes. They analyzed the effect of the thermally dependent viscosity on different quantities and statistics. They reported that the reduction of the consistency near the heated wall induces a radial shift of the fluid particles, from the pipe center towards the wall, due to a high acceleration near the wall and a deceleration in the core region of the pipe. The evolution of the heat transfer coefficient is determined in the different regimes showing the effects of the rheological properties. LES of turbulent flows and heat transfer of thermally dependent power law fluids in a heated pipe were also carried out by Gnambode [7]. He focused on the effects of various parameters (flow index, Reynolds, Prandtl and Pearson numbers) on the statistics and found a significant reduction of the friction factor and Nusselt number with increasing Pearson number.

The objective of this work is to numerically investigate by LES, with an extended Smagorinsky model implemented in a laboratory code developed during Gnambode's PhD thesis [7], the turbulent heat transfer in the fully developed pipe flow of an incompressible power law fluid at n=0.75 and Re_s=4000. The aim is to gain more insights into such complex fluid flows where the viscosity of the fluid is a function of both the temperature and the shear rate. The paper is organised as follows: section 2 introduces the governing equations and the numerical method. Section 3 presents and discusses the LES predictions. The main conclusions are drawn in section 4.

2. Material and methods

2.1. Governing equations

The present study deals with the fully developed turbulent flow and heat transfer of power law fluids in pipes whose wall is heated at a constant heat flux φ_p. The filtered non-newtonian equations are made dimensionless using the centreline axial velocity of the analytical fully developed laminar profile, $U_{cL} = (3n+1)U_b/(n+1)$, where U_b is the average velocity, the pipe radius, R, and the reference temperature, $T_{ref} = \varphi_p R/\lambda$, where λ is the fluid thermal conductivity, as velocity, length and temperature scales respectively. These filtered equations can be expressed as follows:

$$\frac{\partial \overline{u_i}}{\partial x_i} = 0 \tag{1}$$

$$\frac{\partial \overline{u_j}}{\partial t} + \frac{\partial \overline{u_i}\,\overline{u_j}}{\partial x_i} = -\frac{\partial \bar{P}}{\partial x_j} + \frac{1}{Re_s}\frac{\partial}{\partial x_i}\left[\overline{\gamma^{n-1}}\left(\frac{\partial \overline{u_j}}{\partial x_i} + \frac{\partial \overline{u_i}}{\partial x_j}\right)\right] + \frac{\partial \overline{\tau_{ij}}}{\partial x_i} \tag{2}$$

$$\frac{\partial \overline{\Theta}}{\partial t} + \frac{\partial}{\partial x_j}\left(\overline{u_z}\,\overline{\Theta} - T_{\Theta j}\right) - \overline{u_z}\frac{d}{dz} < T_w >= \frac{1}{Re_s\, Pr_s}\frac{\partial^2 \overline{\Theta}}{\partial x_k\, \partial x_k} \tag{3}$$

where the dimensionless temperature is defined by:

$$\Theta = \frac{< T_w(z) > - T(\theta, r, z, t)}{T_{ref}} \tag{4}$$

where T_w is the wall temperature and < > is an average in time and periodic directions. The subgrid heat flux tensor $T_{\theta j}$ is defined and estimated by :

$$T_{\Theta j} = \overline{\Theta u_j} - \overline{\Theta}\,\overline{u_j} = -\alpha_t \frac{\partial \overline{T}}{\partial x_j} \tag{5}$$

where $\alpha_t = \nu_t / Pr_t$ is the thermal diffusivity and Pr_t is the turbulent Prandtl number which is constant for a given flow index n. Indeed, preliminary LES simulations carried out with the dynamical model [2, 7] allowed to estimate Pr_t: for n=1, Pr_t=0.7 and for n=0.75, Pr_t =1.5. The Reynolds and Prandtl numbers of the simulations are defined as $Re_s = \rho U_{cL}^{2-n} R^n / K_0$ and $Pr_s = K_0 / \rho \alpha R^{n-1} U_{cL}^{n-1}$ respectively (α being the thermal diffusivity and ρ the density). The apparent viscosity η of the fluid is modeled by a power-law (Ostwald de Waele model) given by $\eta = K\gamma^{n-1}$, where $K = K_0 \exp[Pn(\Theta - \Theta_b)]$, K_0 is the consistency at the bulk temperature T_b, $Pn = bT_{ref}$ is the Pearson number and b is the parameter of the thermo-dependence. $\gamma = \sqrt{S_{ij}S_{ij}}$ is the shear rate, with the strain rate tensor $S_{ij} = (u_{i,j} + u_{j,i})/2$.

2.2. Dynamic eddy viscosity model

The subgrid stress tensor $\overline{\tau_{ij}}$ is linked to the strain rate tensor $\overline{S_{ij}}$ by $\overline{\tau_{ij}} = -2\nu_t \overline{S_{ij}}$. In the non-newtonian Smagorinsky model by Ohta and Miyashita [1], the turbulent viscosity is computed by $\nu_t = C_s f_s (f_n \Delta)^2 \overline{S_{ij}}$, where Δ is the computational filter, C_s the model constant, f_s the van Driest wall damping function, and f_n the correction function for the change in viscosity. Note that when the spatial filter is applied to the Navier–Stokes equations, in non-newtonian viscous fluid flows (with spatially varying viscosity characteristics), additional terms are derived because the stress tensor is a non-linear function of the strain rate tensor. This

means that in the current LES study with a standard dynamic model, the additional terms are ignored. Indeed, it has been shown by Ohta and Miyashita [1] that these terms are much smaller than the sub-grid scale (sgs) stress. These authors demonstrated this result by comparing the profiles of the sgs stress and of the additional terms estimated from a filtering of the DNS results for power-law fluids. Therefore, in their study, Ohta and Miyashita [1] concentrated on a modification of the sgs model for the viscosity characteristics of non-newtonian fluid and ignored the additional terms.

2.3. Numerical procedure

The above mathematical model was implemented in a finite difference laboratory code. The governing equations were discretized on a staggered grid in cylindrical coordinates. The numerical integration was performed by a finite difference scheme, second-order accurate in space and time. The time advancement was based on a fractional step method. A third-order Runge-Kutta explicit scheme and a Crank-Nicolson implicit scheme were used to evaluate the convective and diffusive terms, respectively. Uniform computational grid and periodic boundary conditions were applied to the circumferential and axial directions. Non-uniform meshes specified by a hyperbolic tangent function were employed in the radial direction. Different grids have been tested for n=0.75 and 1 and predictions were compared to those of the literature. The grid 65^3 was found to provide an accurate prediction of the turbulence statistics, in agreement with the available data of the literature, and to give a good compromise between the required CPU-time and accuracy. Detailed validations for isothermal flows can be found in [2, 7]. The statistics are computed by averaging in the periodic directions and in time.

3. Results and discussion

It is difficult to validate the present non-isothermal LES predictions because the literature survey indicates that there are few works devoted to turbulent thermal field and heat transfer in non-newtonian fluid flows. First the present LES predictions are validated by comparison to the results of the non-thermally dependent fluid case, for both laminar and turbulent flows, before dealing with the thermally-dependent case which is more complex. In that aim, we performed simulations of the laminar and turbulent heat transfer of non-thermally dependent pipe flows at Pr_s=1, Re_s=4000 and various flow indices. Then, we investigated the effects of the Reynolds and Prandtl numbers on the statistics for both shear-thinning and shear-thickening fluids. The reader can find the detailed validations in Gnambode [7]. We shall present here only some of them: the comparison of the velocity predictions at Pn=0 to the universal laws for n=1 and the comparison of the predicted turbulent friction factor and Nusselt number to the available correlations of literature. Then, in the following sections, main emphasis is placed on the Pearson number effects on the turbulent flow and thermal fields.

3.1 Mean velocity and temperature profiles

Our LES results for the mean axial velocity profiles scaled by the friction velocity, $U^+ = U/U_\tau$ with $U_\tau = (\tau_w/\rho)^{1/2}$ and τ_w the wall shear stress, are plotted in figure1a versus the distance to the wall $y^+ = \rho U_\tau (r-R)/\eta_w$, where η_w is the mean wall viscosity. With increasing the Pearson number, Pn, the fluid flow is accelerated in the log-region, Fig.1a. Indeed, the

viscosity for the newtonian fluid (n=1) is equal to the consistency, $\eta = K$. Since Pn>0 and $\Theta - \Theta_b = T_b - T$ is negative near the wall, the consistency $K = K_0 \exp[Pn(\Theta - \Theta_b)]$ decreases when approaching the wall. This means that the viscosity η is smaller near the wall at $Pn \neq 0$, leading to a faster flow in the buffer and log regions, Fig.1a. For the shear-thinning fluid (n=0.75), the viscosity is equal to $\eta = K\dot{\gamma}^{-0.25}$ and its viscosity near the wall is lower than that for n=1. Consequently, the enhancement of the velocity in the buffer and log regions at Pn=1 is more pronounced for n=0.75 in comparison to the newtonian case. Because the fluid flow is more accelerated for n=0.75 at Pn=1, its temperature T is significantly reduced towards the pipe centre. This is clearly visible in figure 1b where the dimensionless temperature Θ increases towards the core region, for n=0.75 at Pn=1, due to the decrease of T, because the residence time of the fluid particles in the channel is smaller.

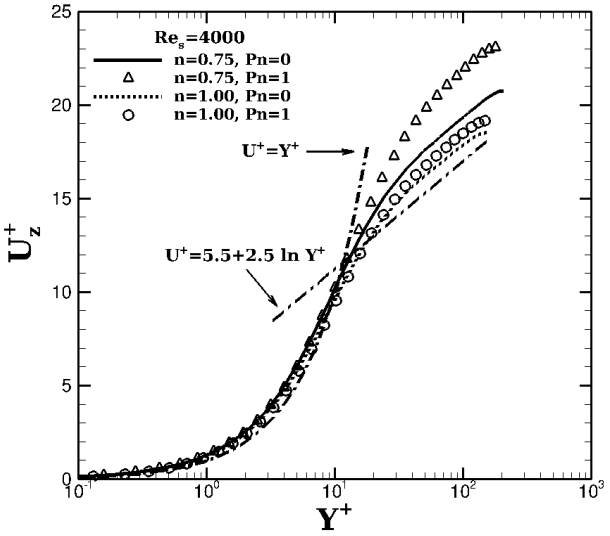

Figure 1a. Axial mean velacity profile, Pr_s =1

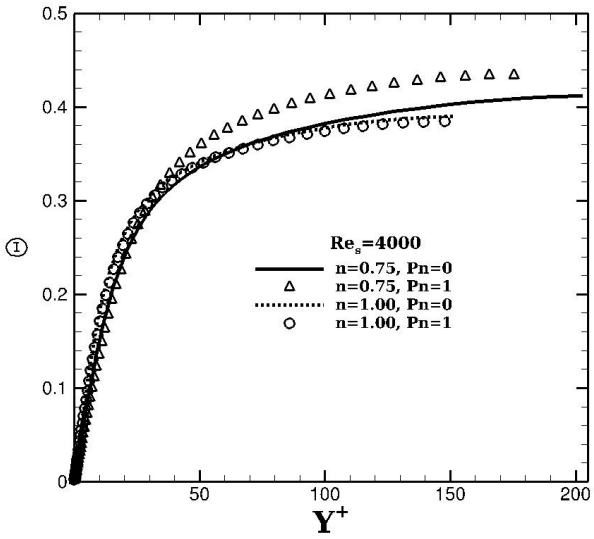

Figure 1b. Mean temperature profile, Pr_s =1

3.2 Mean normalized viscosity

The distribution of the shear rate versus the radial coordinate is depicted in figure 2a. It clearly exhibits a smaller shear rate in the core region of the pipe and a higher one near the wall. The shear rate near the wall is higher for $n = 0.75$. The variation of the mean viscosity is plotted in figure 2b to give further insights into the flow field. For the newtonian fluid, the viscosity is constant when Pn=0 because $\eta = K_0$. For a given n, figure 2b clearly displays a higher viscosity towards duct center with increasing Pn, especially for n=0.75. With increasing Pn, the viscosity increases when approaching the core region of the pipe because $\Theta - \Theta_b = T_b - T > 0$ and the consistency increases: the fluid becomes more rigid. For the shear-thinning fluid, at $Pn = 0$, the viscosity near the wall, Fig.2b, is smaller than that for $n = 1$, since $\dot{\gamma}(n = 0.75) > \dot{\gamma}(n = 1)$ in this region, Fig.2a. The viscosity is enhanced towards the pipe center when increasing Pn, Fig.2b, due to the shear-thinning property combined with the increasing consistency.

3.3 Friction factor and Nusselt number

To validate the present computations, the friction factor and the Nusselt number are compared to the results reported in the literature. They are found to agree fairly well with them. For n=0.75, the predicted friction factor, $f = 2\tau_w / (\rho U_b^2)$, are in accuracy ranges of

10%, 11.4% and 20% compared with the correlations by Oswald de Waele and Gomes (Eq.18 in [9]), Hanks and Ricks [10] and Dodge and Metzner (Eq.17 in [9]), respectively, Table 1. These results clearly show that the friction factor decreases for a decreasing n, at a given Re_s.

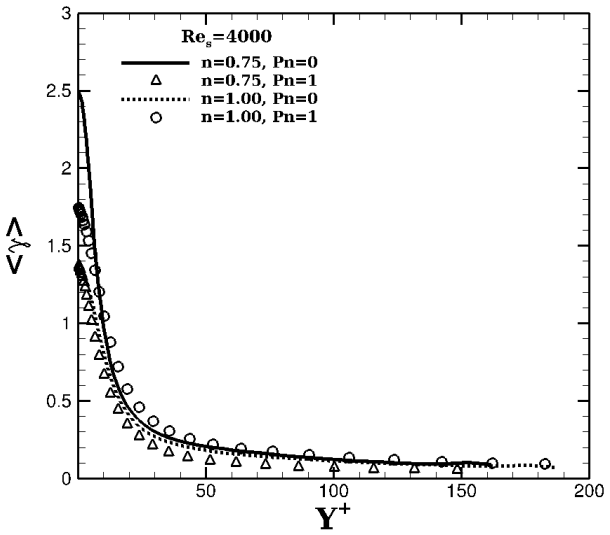

Figure 2a. Shear rate profile, $Pr_s = 1$

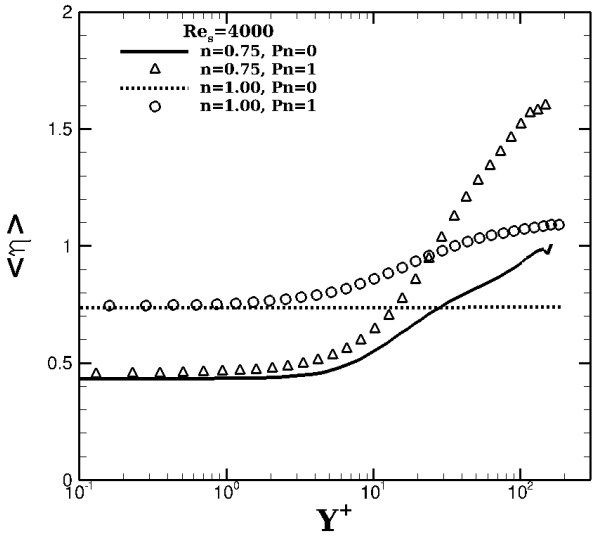

Figure 2b. Mean viscosity profile, $Pr_s = 1$

For n=0.7, the present Nusselt number, defined by Nu=hD/k with $h = -k(\partial\overline{T}/\partial r)_w$, is close to the numerical prediction by Quaresma [3] within a 0.2% accuracy for Pr_s=11 and a 2% accuracy for Pr_s=100, Table 2. The agreement is also satisfactory with the correlation by Pinho and Coelho [11]. The Nusselt number deviates however from the correlation by Sandall et al. [12] within 61% for Pr_s=11 and 80% for Pr_s=100. We can conclude that this correlation seems not valid for high Prandtl numbers. For n=0.75 and 1, at Re_s=4000, a reduction of the friction factor and Nusselt number is observed with increasing Pn, Table 3. This reduction is significant at n=0.75. However note that, at Pn=0, when n decreases, the Nusselt number increases, while it decreases at Pn=1, Table 3.

Table 1. Friction factor at $Pr_s = 1$, Pn=0 and $Re_s = 4000$.

n	Present LES	Dodge and Metzner [9]	Oswald de Waele & Gomes [9]	Hanks & Ricks [10]
0.75	9.12×10^{-3}	7.60×10^{-3}	8.24×10^{-3}	8.18×10^{-3}
1.0	10.47×10^{-3}	8.68×10^{-3}	9.99×10^{-3}	9.73×10^{-3}
1.2	10.94×10^{-3}	9.45×10^{-3}	11.27×10^{-3}	10.81×10^{-3}

Table 2. Nusselt number at $Pr_s = 1$, Pn=0 and $Re_s = 4000$.

n	Pr_s	Present LES	Quaresma [3]	Sandall & al. [12]	Pinho & Coelho [11]
0.7	100	109.69	111.94	60.77	96.43
0.7	11	45.41	45.30	28.18	45.21
1.0	1	18.45		24.99	18.30
1.2	1	17.55		22.48	14.77

Table 3. Friction factor and Nusselt number at $Pr_s = 1$ and $Re_s = 4000$ for the present LES.

	n=0.75		n=1	
	Pn=0	Pn=1	Pn=0	Pn=1
$f\times10^3$	9.12	6.99	9.49	9.11
Nu	20.19	15.07	18.45	17.86

3.4 Root mean squares of turbulent fluctuations

As shown in Fig. 3a, the profiles of the root mean square (rms) of the fluctuating axial velocity, U_z', of the newtonian fluid (n=1) for Pn=0 and Pn=1 are nearly the same: a very small increase of the rms at Pn=1 is observed on a part of the pipe section between r/R=0.2 and r/R=0.9. On the other hand, the rms U_z' of the shear-thinning fluid (n=0.75) for Pn=1 exhibits higher values than for Pn=0, between the pipe axis and r/R=0.9, Fig. 3a. Its profile peak slightly increases and moves far away from the wall with increasing Pn. On the contrary, the rms of the radial and azimuthal velocity fluctuations are much more low for Pn=1 than for Pn=0, Fig. 3b,c. The higher intensity of the rms of $U_z'^+$ at Pn=1 is due to the higher value of the velocity U_z^+ in the buffer and log regions, Fig. 1a. In the core region, for $Y^+>20$ (r/R<0.7), Pn has no impact on the value of turbulent kinetic energy (not shown here). Thus, the augmentation of the rms of U_z' at Pn=1 leads to a diminution of the rms of U_r' and U_θ' in this region. The rms of the temperature Θ'^+ for Pn=1, just like the rms of $U_z'^+$, is enhanced between the pipe axis and r/R=0.9, Fig. 3d. However, the rms of the fluctuating temperature is much lower than the rms of the fluctuating velocities. The peaks of the rms of Θ'^+ at Pn=0 (for both n=0.75 and n=1) are higher and located closer to the wall than for the case of the thermally dependent fluid (Pn=1). Thus the fluctuations of the temperature are less intense in the vicinity of the wall with increasing Pn.

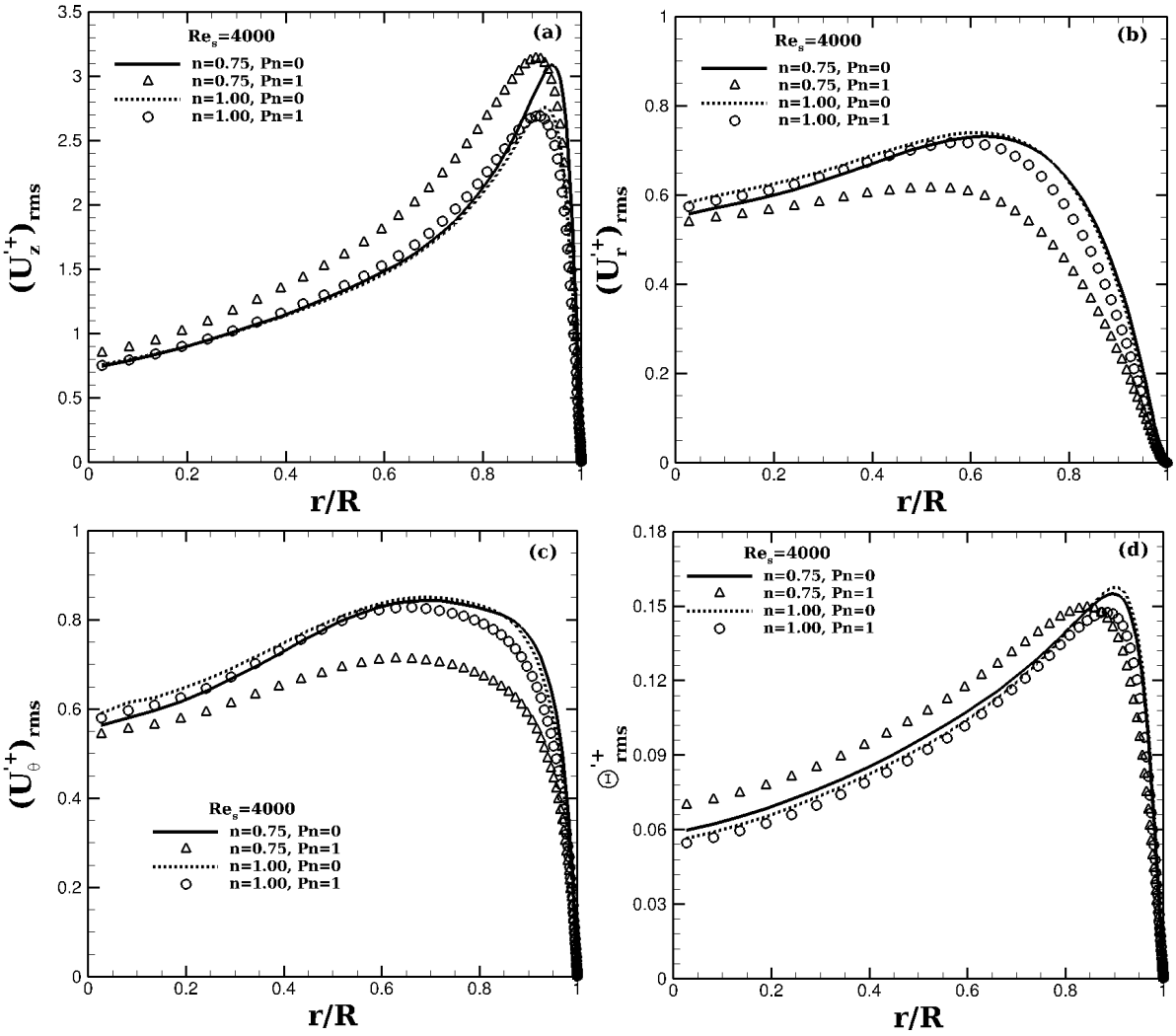

Figure 3. Root mean square of the fluctuating velocities and temperature, $Pr_s = 1$.

3.5 Reynolds stress and turbulent heat fluxes

Figures 4.a,b depict the profiles of turbulent radial and axial heat fluxes. The turbulent axial heat flux, presented in Fig.4b, behaves like the rms of the fluctuating axial velocity, Fig.3a, showing a strong correlation between the fluctuations Θ' and U_z'. The turbulent radial heat flux undergoes a noticeable reduction with increasing Pn, because the fluid viscosity grows towards duct center when Pn increases. The Reynolds shear stress profile behaves like the turbulent radial heat flux when Pn varies (not shown here). Its distribution is shifted far from the wall with increasing Pn, and its peak value is noticeably reduced.

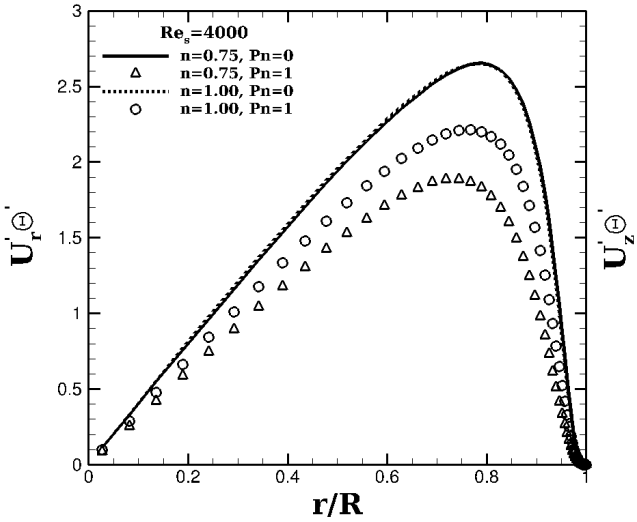

Figure 4a. Turbulent radial heat flux, Pr_s =1

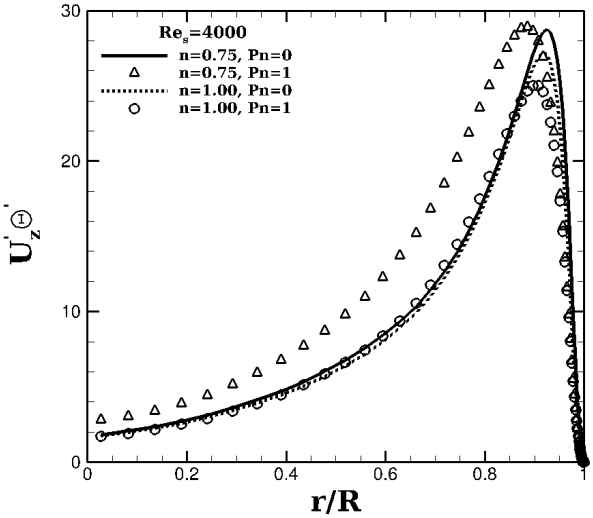

Figure 4b. Turbulent axial heat flux, Pr_s =1

3.6 Visualizations

To explore the effects of the Pearson number on the flow, the resolved axial velocity fluctuations are presented in Fig. 5. For the newtonian fluid (n=1), with increasing Pn, the turbulent structures are less random and the streaks are larger indicating a less developed turbulence. For the shear-thinning fluid (n=0.75), the number of streaks is reduced compared with the newtonian case and much longer streaks appear, particularly at Pn=1, suggesting a reduction of turbulence and, as a consequence, of the heat transfer. The reduction of turbulence is more pronounced at n=0.75, due the augmentation of the viscosity towards the pipe center, Fig.2b.

4. Conclusions

This study is the first contribution that allows to check the applicability of LES, with an extended Smagorinsky model, to the turbulent flows and heat transfer of thermally dependent power-law fluids in pipes. The LES results allowed to gain more insight into these complex fluid flows with shear rate and temperature dependent viscosity. In the present LES of fully developed turbulent flow of power law fluids in heated pipes, under isoflux conditions, the Pearson number effects on flow and thermal fields have been revealed. For the non-thermally dependent viscosity case (Pn=0), the LES axial velocity profile for the shear-thinning and newtonian fluids, as well as the friction factor and Nusselt number, are in reasonably good agreement with the findings of the literature. With increasing Pn (thermally dependent viscosity case), the mean viscosity is enhanced towards the pipe center. This leads to a

diminution of the turbulent radial heat flux and an acceleration of the flow in the log-region where the temperature is slightly reduced. As a consequence, the friction factor and the Nusselt number undergo a significant reduction when Pn increases. With increasing Pn, the rms of $U_z'^+$ and Θ'^+ are almost the same for the newtonian fluid (n=1) but they are noticeably enhanced between the pipe center and r/R=0.9 for the shear thinning fluid (n=0.75).

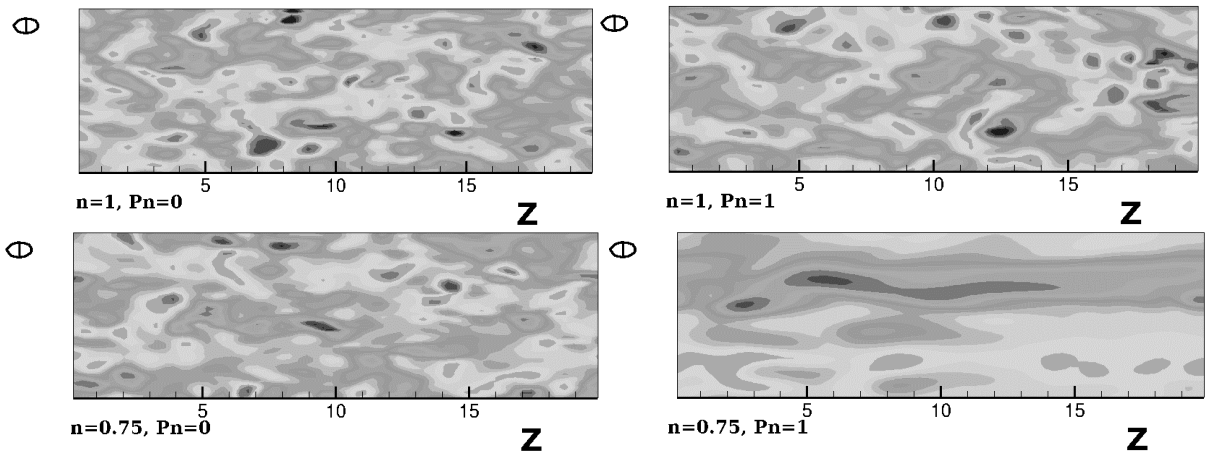

Figure 5. Resolved axial velocity fluctuations at $Y^+ \approx 15$

5. References

[1] T. Ohta, M. Miyashita, DNS and LES with an extended Smagorinsky model for wall turbulence in non-Newtonian viscous fluids. J. Non-Newton. Fluid Mech. 206 (2014) 29-39.

[2] P. S. Gnambode, P. Orlandi, M. Ould-Rouiss, X. Nicolas, Large-Eddy simulation of turbulent pipe flow of power-law fluids, Int. J. Heat Fluid Flow 54 (2015) 196-210.

[3] J. N. N. Quaresma, J. A. Lima, Thermally developing turbulent flow of pseudoplastic fluids within circular tubes. Int. Comm. Heat Mass Transfer 25 (8) (1998) 1105-1114.

[4] P. S. Gnambode, P. Orlandi, M. Ould-Rouiss, X. Nicolas, LES des transferts thermo-convectifs dans l'écoulement turbulent d'un fluide d'Ostwald de Waele en conduite cylindrique chauffée. 22ème Congrès Français de Mécanique, Lyon, France, 2015.

[5] V. Scirocco, R. Devienne, M. Lebouche, Ecoulement laminaire et transfert de chaleur pour un fluide pseudo-plastique dans un tube. Int. J. Heat Mass Transfer 28 (1) (1985) 91-99.

[6] J. Peixinho, Contribution expérimentale à l'étude de la convection thermique en régime laminaire, transitoire et turbulent pour un fluide à seuil en écoulement dans une conduite, PhD thesis, Université Henri Poincaré Nancy 1, France, 2004.

[7] P. S. Gnambode, Simulation des grandes échelles des transferts thermo-convectifs dans les écoulements turbulents d'un fluide non-newtonien en conduite cylindrique, PhD thesis, Université Paris-Est Marne-la-Vallée, France, 2015.

[8] M. Rudman, H. M. Blackburn, L. J. W. Graham, L. Pullum, Turbulent pipe flow of shear-thinning fluids. J. Non-Newtonian Fluid Mech. 118 (2004) 33–48.

[9] F.J.A.D. Gomes, Hydraulic, power-law models, calculation method using ... Technical meeting on software developing in drilling operations, CAPER/87, Salvador, Brazil, 1987.

[10] R. W. Hanks, B. L. Ricks, Transitional and turbulent pipe flow of pseudo-plastic fluids, J. of Hydronautics 9 (1975) 39-44.

[11] F. T. Pinho, P. M. Coelho, Non-newtonian heat transfer. CEFT/DEMec, Faculdade de Engenharia Universidade do Porto Portugal, 2010.

[12] O. C. Sandall, O. T. Hanna, K. Amarnath, Experiments on turbulent non-newtonian mass transfer in a circular tube. AIChE J. 32 (12) (1986) 2095-2098.